J Solid State Electrochem (2016) 20:1175–1180
DOI 10.1007/s10008-015-2944-2

ORIGINAL PAPER

Polyaniline nanostructure electrode: morphological control by a hybrid template

Carlos P. Silva [1] · Mireya Santander-Nelli [1] · Cristian Vera-Oyarce [1] · Juan F. Silva [1] · Alejandra Gómez [1] · Lisa A. Muñoz [1] · José H. Zagal [1] · Miguel Gulppi [1] · Jorge Pavez [1]

Received: 28 April 2015 / Revised: 22 June 2015 / Accepted: 24 June 2015 / Published online: 11 July 2015

Abstract We report here a novel approach to the template-assisted electrochemical synthesis of vertically aligned polyaniline (PANI) nanostructure surface arrays. When PANI is obtained by electropolymerization inside a custom-made anodic aluminum oxide (AAO) template, with an Au layer sputtered onto one side of the AAO acting as an anode, PANI nanotubes are obtained. In contrast, when the surface of this gold layer is modified with 4-aminothiophenol (4-ATP) as a self-assembled monolayer (SAM) film anchored to the gold layer via the thiol groups and on the opposite end having NH_2 functionalities, we obtain a surface array of PANI nanowires. Cyclic voltammetry and SEM analysis show that the amino functionalities of Au/SAMs act as a nucleation site in the internal base of the AAO pore and determine both the morphology and structure of polyaniline and its electronic properties as well.

Keywords Polyaniline · Template · AAO · SAMs · Electropolymerization · Nanostructured

Introduction

Polyaniline (PANI) is one of most profusely studied conducting polymers from both the fundamental and applied aspects, especially because it is easily obtained and it is highly stable [1]. Nanostructured PANI shows advantages over the conventional bulk polymer because it has a much higher surface area available and possesses special electronic properties. Various chemical and electrochemical synthetic approaches have been reported for obtaining this material. For instance, nanostructured PANI has been mainly fabricated using template methods, which make use of inorganic materials, such as anodic aluminum oxide (AAO) [2] and organic molecules [3, 4] or polymers which are the most commonly used materials as molecular templates for the fabrication of PANI nanostructures [5–8]. The special features of systems containing self-assembled monolayers (SAMs) on metallic surfaces have inspired several studies where the organic assembled layers are used as templates for directing the growth of PANI, improving the control of its morphology and its electrochemical properties [7, 9, 10]. Rubinstein and Shannon have reported pioneering work using 4-aminothiophenol (4-ATP) [11, 12] and mixed monolayers of 4-ATP and *n*-octadecanothiol (ODT) [13, 14]. Rubenstein's work was based on the chemical resemblance between 4-ATP and aniline and established that this aspect plays a key role in the control of the morphology of PANI. Meanwhile, Shannon has proposed that starting from a certain 4-ATP/ODT ratio value, a phase separation of thiols is observed and a growth of nanostructured PANI takes place on the 4-ATP islands formed within an ordered ODT. Because the pore dimensions of an AAO membrane (length and diameter) can be easily controlled, this makes this material very attractive for template synthesis of various nanomaterials [2, 15, 16]. Commonly, AAO has been used as a template for the electrochemical and electroless deposition of PANI [7, 17, 18]. Thus, here, we present a new strategy that combines the AAO membrane as an inorganic template with an organic one (4-ATP) to achieve the electrochemical synthesis of PANI nanostructures with a high control of its morphology.

✉ Carlos P. Silva
carlos.silvamo@usach.cl

✉ Jorge Pavez
jorge.pavez@usach.cl

[1] Departamento de Química de los Materiales, Facultad de Química y Biología, Universidad de Santiago de Chile, Av. Libertador B. O'Higgins 3363, Casilla 40, Correo 33, Santiago, Chile

Experimental

Materials

All chemicals and solvents were of reagent grade; 4-ATP (Aldrich) was used as received and aniline (Aldrich) was distilled over zinc powder before use. Aluminum was used as foils (99.999 %, Goodfellow). Electrochemical data were obtained using an AUTOLAB Potentiostat and a three-compartment electrochemical cell. A Cl^--saturated Ag/AgCl (Bioanalytical System) electrode was used as reference, and a platinum (99.99 %, Aldrich) spiral wire served as the auxiliary electrode. The AFM images were obtained with a Nanoscope IIIa (Veeco). SEM analysis was performed on a LEO 1550 FESEM (Keck SEM).

Preparation and characterization of the AAO template

The synthesis of the AAO template was carried out by a two-step anodizing process as suggested by Masuda et al. [19]. High-purity Al foils were used as starting material. The Al foils were degreased with acetone and further annealed under an argon atmosphere at 400 °C for 3 h. Thereafter, the foils were electropolished in a mixture of perchloric acid ($HClO_4$) and ethanol (1/4 *v*/*v*) by applying a constant voltage of 20 V at 5 °C for 5 min under stirring in order to reduce the surface roughness. The anodizing procedure was carried out at 40 V in 0.3 M $H_2C_2O_4$ at 20 °C. The first and second anodizing steps were performed under the same conditions, but before proceeding with the second anodization step, the porous alumina was removed by etching in a solution containing a mixture of phosphoric and chromic acids. After finishing both anodizing steps, the Al was dissolved in a $CuCl_2$/HCl mixture solution. A gold-sputtered layer that acted as host for 4-ATP SAMs was added on the top face of the AOO template. Silver epoxy was used to attach a Cu wire to the gold layer, and finally, the base of the template was covered with epoxy resin. The AAO membranes were characterized using AFM and SEM.

Synthesis of SAMs using 4-ATP

The functionalization of the surface of the gold-sputtered layer at the bottom of the pores of AAO was carried out by the formation of SAMs of 4-ATP molecules bearing the amino at the outermost portion of the SAM layer. The AAO/gold-sputtered layer was submerged in a solution of 4-ATP 50 μM in ethanol to incubation for 12 h. The hybrid template so obtained was washed with ethanol and dried in a N_2 stream. The SAM formation was characterized by cyclic voltammetry performing electrodesorption curves in NaOH electrolyte.

Electropolymerization of aniline

The electropolymerization of aniline in both the AAO and AAO/4-ATP hybrid templates was carried out by potential cycling of the electrode between 0.0 and +1.0 V at a scan rate of 0.05 V/s. The electrolyte was 1 M HNO_3 in water and containing 50 mM of aniline. As concerns the electrosynthesis method and according to the aim of this work, we chose the potentiodynamic polymerization as the synthesis method because, according to literature [7], the potentiostatic one would be able to affect the morphology of PANI nanostructures interfering in the study of the morphologic control by the hybrid template on the electropolymerization of PANI. Furthermore, the potentiodynamic method offers us better conditions to control the rate of filling of the pores with the growing polymer. In relation to galvanostatic method, production of a lower quality polymer due to the degradation reactions that take place is more significant with these methods than the potentiodynamic one, affecting the polymer morphology notoriously [7].

Results and discussion

Characterization of the AAO/4-ATP hybrid template

Figure 1a shows a SEM image of the AOO film surface prepared by the two-step anodization procedure in 0.3 M $H_2C_2O_4$ electrolyte. The SEM image clearly shows the very large hexagonal self-ordered porous array of the AAO template membrane. Prior to etching the barrier layer of AAO with 5 % H_3PO_4 solution, the hexagonal cell parameters (pore diameter and interpore distance) were obtained by cross section analysis of the AFM images that showed a pore diameter of 61± 5 nm and an interpore distance of 108±5 nm (see the inset in Fig. 1a). Figure 1b shows the electrochemical characterization using cyclic voltammetry of 4-aminothiophenol SAMs built up on the gold layer at the inner base of the pores of the AAO template. The reductive desorption process of the SAMs in 0.1 M NaOH at 0.05 V/s shows a principal peak at −0.8 V, which is typical of thiol used here, indicating a one-electron transfer for the desorption of the 4-ATP from the gold surface [20]. Two additional more negative broad weak peaks are observed in the voltammetric profile, indicating the electrodesorption of 4-ATP molecules from other kinds of surface domains or from surface defects of the polycrystalline gold layer at the inner base of the AAO pores. The inset of Fig. 1b shows the voltammetric response in 0.1 M $HClO_4$ electrolyte of the 4-ATP anchoring layer after a few scans at 0.05 V/s. The voltammetric profile shows a single reversible redox process centered at 0.52 V whose peak current exhibited a linear behavior with the potential scan rate, which is indicative that this redox process is due to a species anchored to the

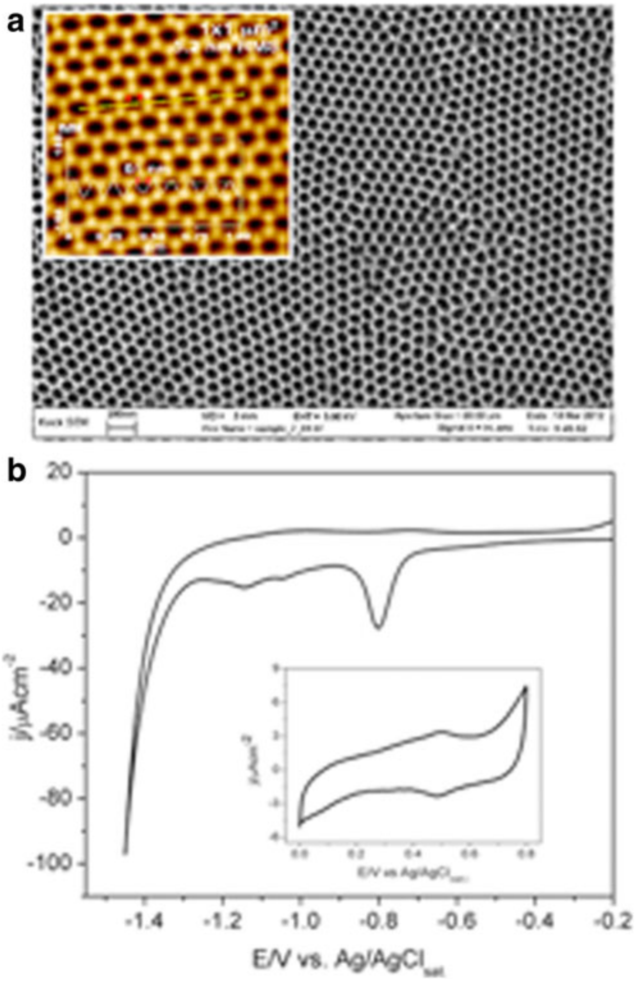

Fig. 1 **a** SEM image of the AAO template. **b** Electrodesorption curve in basic media of 4-ATP SAMs in the hybrid template. The *inset* of **b** shows the final voltammetric response of 4-ATP in 0.1 M $HClO_4$ at the hybrid template

gold surface electrode. This process has been assigned to the *p*-benzoquinone/hydroquinone couple produced by the oxidation of 4-ATP to a radical cation followed by dimer formation by a chemical bond [12, 14]. This voltammetric response confirms the 4-ATP SAM formation inside the pores of AAO and shows that the hybrid template is indeed obtained.

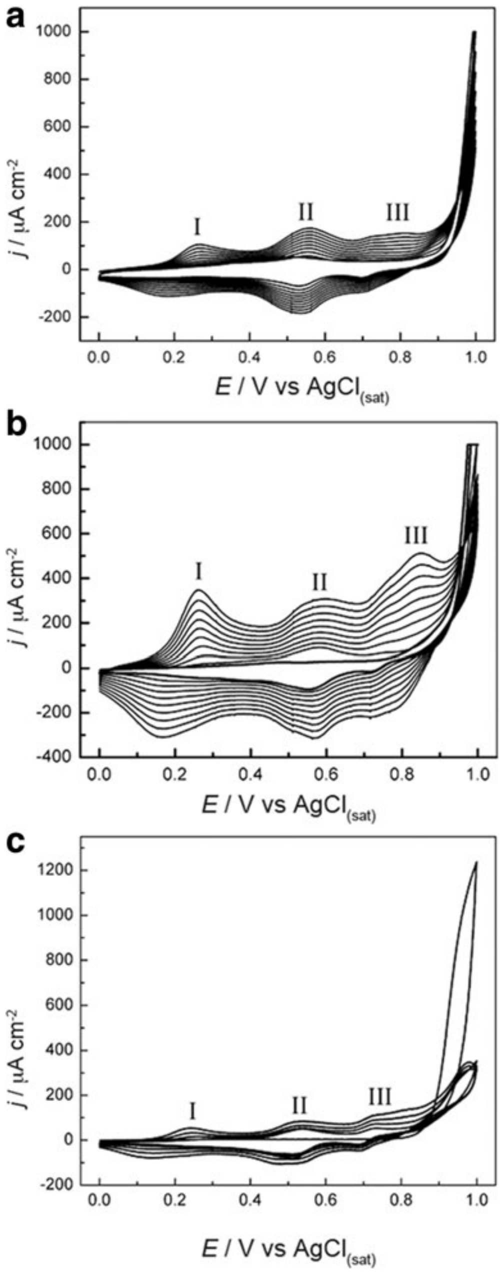

Fig. 2 Potentiodynamic electropolymerization of aniline in **a** the AAO template, **b** the AAO/4-ATP hybrid template, and **c** the bare gold electrode. Electrolyte: 1 M HNO_3 containing 50 mM of aniline. Potential scan rate: 0.05 V/s

Electropolymerization of aniline in the AAO and AAO/4-ATP hybrid templates

The electropolymerization of aniline was accomplished within the pores of both the AAO (Fig. 2a) and hybrid templates (Fig. 2b) by cycling the potential of the electrode between a lower limit of 0.0 V and an upper limit of +1.0 V at a scan rate of 0.05 V/s. According to previous antecedents, we chose to use ten potential cycles to grow the PANI nanostructure because the effect of 4-ATP on aniline polymerization takes place and becomes evident in the voltammetric response at the earlier stage of PANI growth.

The electrolyte was 1 M HNO_3 containing 50 mM of aniline. As a reference system, we also performed the electropolymerization of aniline on a massive gold electrode (Fig. 2c) at the same conditions used for the previous case. As it is observed in the three systems in Fig. 2, by repetitive cycles of potential, the typical gradual rise in the current peak is observed, reflecting the deposition of an electroactive PANI film on the electrode surface. As observed for the series of repetitive voltammograms, only after the second cycle are redox processes observed, with the peak currents continuously growing with the successive potential cycles. Peak I corresponds to the first oxidation of the neutral PANI film; process III corresponds to the fully oxidized form of PANI, the emeraldine/pernigraniline couple; and process II has been attributed to the presence of polymer structures with a high degree of network crosslinking, induced by a monomer attached at *ortho*-position of the aromatic ring on the main chain during the elongation stage [21]. The similarity of the these three voltammetric profiles regarding the redox processes observed during the electropolymerization process confirms the growth of the polyaniline in the three systems represented in Fig. 2.

The cyclic voltammetric response of the first electropolymerizing cycle of aniline in both the AAO and hybrid templates is shown in Fig. 3a. The voltammogram in black (AAO template) does not show any visible oxidation process below 0.9 V, and beyond this value, an irreversible intense redox process appears which is assigned to the formation of the radical-cation anilinium ($C_6H_5NH^{*+}$) which can be formed from the oxidation of the aniline monomers at the vicinity of the electrode surface. This anilinium radical is stabilized by resonance [22] and a rapid coupling process of radicals takes place which leads to the formation of the dimer *p*-aminodiphenylamine (ADPA), and thereafter, the polymer growth process continues to progress [21–23]. In contrast, the profile of the first electropolymerizing cycle of aniline in the hybrid template shows a very different shape. The voltammogram in red if Fig. 3a shows a quasi-reversible redox process located between 0.3 and 0.5 V where the anodic wave appears at about 0.3 V less positive than the onset potential of the aniline monomer oxidation wave. This redox process corresponds to the electrooxidation of the amino group of 4-ATP to form the nitrinium radical cation on the electrode surface, as reported in the literature [13, 14]. These results confirm the presence of SAMs of 4-ATP covalently bound to the gold surface inside the nanopore array of AAO. Following the anodic sweep, once the oxidation potential of the aniline monomer is reached, the radical cation anilinium ($C_6H_5NH^{*+}$) is formed. This radical cation then binds to the electrode surface by a head-tail coupling reaction with nitrinium formed from the 4-ATP present in the SAMs to produce the dimer aminodiphenylamine (ADPA) anchored to the surface. In the following anodic sweep, this dimeric unit is oxidized, generating a new reactive radical cation dimer [10, 21]. These observations indicate that the polyaniline growth stage is initiated from the 4-ATP cation radical anchored onto the surface of the gold electrode, and this species seems to be acting as a nucleation site, and then polymerization proceeds from the bottom to the top of the hybrid template pore.

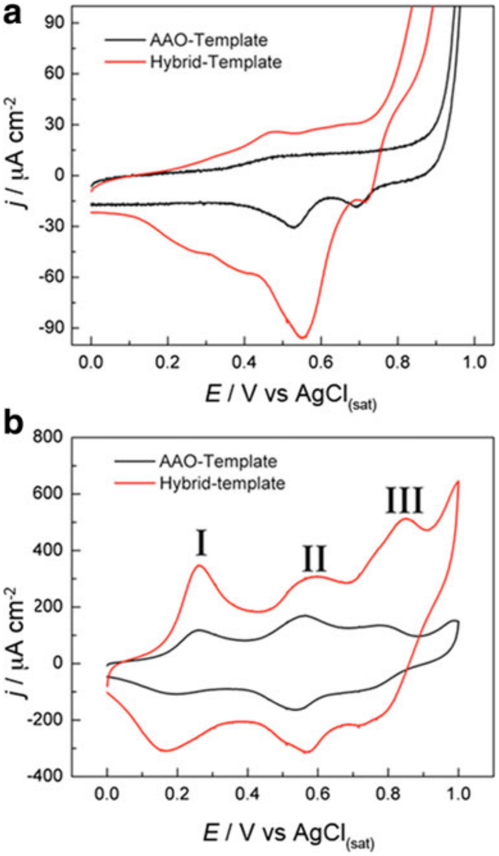

Fig. 3 **a** First potentiodynamic cycling for electropolymerization of aniline in the AAO and hybrid template and **b** cyclic voltammogram of the PANI material, obtained with ten electropolymerizing cycles, in a 1-M HNO_3 monomer-free solution

Figure 3b shows the voltammetric pattern of PANI in acid media electrosynthesized by ten electropolymerizing cycles using the AAO template (black line) and the hybrid template containing the SAMs (red line). Both are typical voltammograms (in a 0.1-M HNO_3 monomer-free solution) for the electropolymerization of PANI and confirm that the electrosynthesis of PANI inside the template's pores was achieved. Even though both polymers were obtained using the same number of electropolymerizing cycles, there are pronounced differences in the peak currents of the three redox processes. Even if one takes into account the capacity exhibited by the polymer films, the peak currents of the redox processes of the polymer obtained using the hybrid template are almost three times those of the polymer obtained when using the AAO template. But the most remarkable feature of both voltammetric profiles is the reversal of peak current values of processes I and III relative to the intermediate peak II. Whereas the peak current of peak II is more intense in the polymer originated from the AAO template, the opposite occurs in the polymer formed from the hybrid template. It has been reported that the maximum conductivity value for the PANI occurs in the potential region between peaks I and III where the polymer evolves from leucoemeraldine (LE)/emeraldine (EM) (peak I) to emeraldine/pernigraniline (PE) (peak III). By subtracting the background current, the charges under oxidation peak I and III are 524.6 and 188.3 μC, respectively, for the hybrid template, whereas for the AAO template, the values are 136.2 and 20.0 μC, respectively, which indicates that the PANI obtained using the hybrid template shows a higher capacitance. In this case, the partially oxidized EM state is the species that possesses the electronic configuration capable of having the charge carriers responsible of the conductivity of the material [24, 25]. It is observed that using the hybrid template for electropolymerization of aniline enhances this feature. On the other hand, the process involved in the middle peak II has been generally attributed to a side reaction (crosslinking) or degradation reactions [23, 24]. The crosslinking process, involving a previous coupling reaction between ADPA-adsorbed dimer units and a monomer radical cation that takes place at early stages during the PANI growth, is associated with thin films of PANI [23]. Whereas, during the potential cycling, the electrochemical degradation of PANI can occur by the formation of quinone species which can undergo oxidation and a subsequent molecular hydrolysis [24]. These reactions have been identified as issues that promote polymer degradation and its passivation with loss of conductivity [24–27]. Thus, we believe that the electropolymerization of aniline is strongly benefitted by the hybrid template regarding its electronic properties.

Morphological characterization of PANI nanostructures

The morphology of the polymer nanostructure surface arrays obtained in both the AAO and hybrid templates was characterized by dissolving the alumina template, by an exhaustive controlled chemical etching with NaOH, right up to when the top of nanostructures was observable. Figure 4 shows the SEM images of PANI obtained in both AAO (Fig. 4a) and in AAO/4-ATP templates (Fig. 4b). It is observed that in both systems, a surface array of nanostructures of PANI is obtained. But, SEM images reveal a remarkable and very interesting difference in the kind of nanostructures of PANI obtained when using the two different templates. By comparing the images, it is observed that the nanostructure of the polymer obtained using the AAO template (Fig. 4a) corresponds to a tubular structure (nanotubes), while for that obtained using the hybrid template, the polymer obtained appears as nanowires. Although in Fig. 4b some PANI open nanostructures are observed, the majority of the population of nanomaterials corresponds to PANI nanowires.

The results shown in Fig. 4a are in agreement with those reported in the literature for these synthesis conditions using AAO as template [2]. The tubular structures seem to arise from the strong interaction taking place between the monomer as a positively charged radical anilinium and the inner wall of the pores of AAO, where there is high local population of oxygenated species rich in available electrons such as −OH, by which an electrophilic addition can occur. This would cause an increase in the local concentration of the monomer (as a radical cation) and active oligomer on the pore walls, thereby promoting the formation of PANI nanotubes that will grow following the direction of the pore walls. Martin et al. observed a similar behavior for the electrosynthesis of gold nanotubes assisted by an AOO template, when the wall pores of alumina were functionalized with cyano groups by silanization [16].

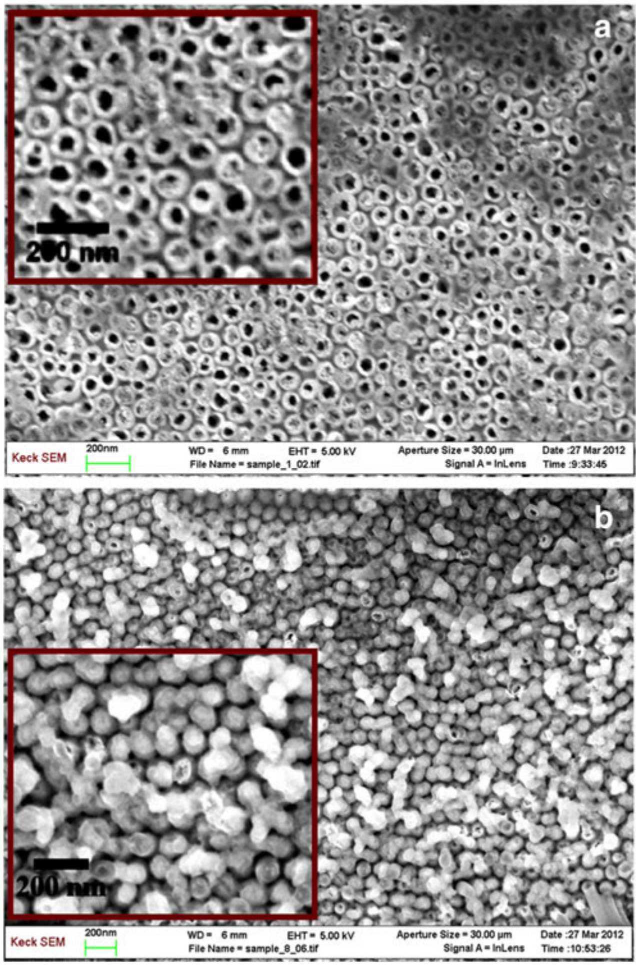

Fig. 4 SEM image of polyaniline electropolymerized in **a** the AAO template and **b** the hybrid template after partial removal of AAO

The preparation of PANI nanowires in the hybrid template involves the phenomenon discussed above related to the presence of 4-ATP as a molecular anchor in the inner base of the alumina pore acting as a nucleation and growth site. After its oxidation during the first anodic sweep, the oxidized 4-ATP SAMs probably provide a better thermodynamic alternative to the oxidized aniline monomer. This reduces its energy by coupling directly to the surface and thereby elongating the polymer chains in the normal direction to the surface and parallel to the pore walls. As a result, a compact structure of PANI nanowires is formed. Similar morphological control was achieved by Park et al. using a gold electrode modified with thiolated aniline monomer, i.e., 4-ATP, as molecular template anchored within β-cyclodextrin cavities [7]. In this template, branched PANI nanowires were obtained when it was grown galvanostatically, and compact wires when the method used was potentiodynamic. In both cases, the 4-ATP within the β-cyclodextrin cavities is considered an initiation site of PANI growth.

Conclusions

In this study, we use a template method for electrosynthesizing PANI nanostructures with an effective control of the morphology, achieved from the use of a hybrid template AAO/SAM 4-ATP. The 4-ATP SAMs built on the internal base of the AAO pore acts as the nucleation site for polymerization. This produces an orientation of the growth of polymer chains within the pore and along the normal direction to the surface and parallel to the pore walls, obtaining thus a compact structure of PANI nanowire surface arrays.

Acknowledgments FONDECYT Grants 1131062, 1140192 and Milllenium Nucleus of Molecular Engineering for Catalysis and Biosensors RC120001 supported this work. CPS and MS-N are thankful to CONICYT for a doctoral fellowship.

References

1. MacDiarmid AG (2001) Angew Chem Int Ed 40:2581–2590
2. Martin CR (1994) Science 266:1961–1965
3. Reginald MP, Martin CR (1986) J Electrochem Soc 133:2206–2207
4. Cao Y, Mallouk TE (2008) Chem Mater 20:5260–5265
5. Ji LY, Kang ET, Neoh KG, Tan KL (2005) Langmuir 18:9035–9040
6. Zhong W, Wang Y, Yan Y, Sun Y, Deng J, Yang W (2007) J Phys Chem B 111:3918–3926
7. Choi SJ, Park SM (2000) Adv Mater 12:1547–1549
8. Xu D, Kang ET, Neoh KG, Tay AAO (2004) Langmuir 20:3324–3332
9. Ulman A (1996) Chem Rev 96:1533–1554
10. Cho SH, Kim D, Park SM (2008) Electrochim Acta 53:3820–3827
11. Sabatani E, Gafni Y, Rubinstein I (1995) J Phys Chem 99:12305–12311
12. Hayes WA, Shannon C (1996) Langmuir 12:3688–3694
13. Hayes WA, Shannon C (1998) Langmuir 14:1099–1102
14. Hayes WA, Kim H, Yue X, Perry SS, Shannon C (1997) Langmuir 13:2511–2518
15. Inguanta R, Piazza S, Sunseri C (2009) Appl Surf Sci 255:8816–8823
16. Martin CR (1995) Acc Chem Res 28:61–68
17. Jani AMM, Losic D, Voelcker NH (2013) Prog Mater Sci 58:636–704
18. Yang SM, Chen KH, Yang YF (2005) Synth Met 152:65–68
19. Masuda H, Fukuda K (1995) Science 268:1466–1468
20. Ponce I, Silva JF, Oñate R, Rezende MC, Paez MA, Zagal JH, Pavez J, Mendizabal F, Miranda-Rojas S, Muñoz-Castro A, Arratia-Perez R (2012) J Phys Chem C 116:15329–15341
21. Pruneanu S, Veress E, Marian I, Oniciu L (1999) J Mater Sci 34: 2733–2739
22. Heinze J, Frontana-Uribe BA, Ludwigs S (2010) Chem Rev 110: 4724–4771
23. Planes GA, Rodríguez JL, Miras MC, García G, Pastor E, Barbero CA (2010) Phys Chem Chem Phys 12:10584–10593
24. Genies EM, Lapkowski M, Penneau JF (1988) J Electroanal Chem 249:97–107
25. Kobayashi T, Yoneyama H, Tamura H (1984) J Electroanal Chem 161:419–423
26. Pournaghi-Azar MH, Habibi B (2007) Electrochim Acta 52:4222–4230
27. Stilwell DE, Park SM (1988) J Electrochem Soc 135:2254–2262